UC Irvine
UC Irvine Previously Published Works

Title

Monitoring freeze—thaw cycles along North—South Alaskan transects using ERS-1 SAR

Permalink

https://escholarship.org/uc/item/3395m3t4

Journal

Remote Sensing of Environment, 49(2)

ISSN

0034-4257

Authors

Rignot, Eric
Way, Jo Bea

Publication Date

1994-08-01

DOI

10.1016/0034-4257(94)90049-3

Copyright Information

Peer reviewed

Monitoring Freeze–Thaw Cycles along North–South Alaskan Transects Using ERS-1 SAR

Eric Rignot[*] *and Jo Bea Way*[*]

Monitoring freeze–thaw cycles of high latitude terrestrial ecosystems is useful for estimating the length of the growing season and annual productivity in the tundra and in boreal forests, for estimating potential damage to living plants due to frost drought, and for evaluating major changes in heat fluxes between land and atmosphere. At microwave frequencies, freezing results in a dramatic decrease of the dielectric constant of soil and vegetation, which significantly alters their radar scattering properties. In this article, we investigate the possibility of monitoring freeze–thaw cycles of terrestrial ecosystems using C-band frequency (5.3 GHz), vertical transmit and receive polarization, synthetic-aperture radar (SAR) data gathered by the European Space Agency's Earth Remote Sensing satellite (ERS-1). Repeat-pass SAR images are mosaicked together along a north–south transect across Alaska, coregistered, and analyzed using a change detection algorithm that determines when the landscape freezes based on a decrease in radar backscatter greater than 3 dB relative to a known thawed, wet state of the landscape. Air-temperature recordings from seven airport weather stations and in situ observations from three monitored forest stands in interior Alaska concur to indicate SAR accurately maps frozen areas across the entire state. The technique does not apply to open water areas because calm water and frozen water are confused. Elsewhere, ERS-1 SAR could monitor thaw/freeze transitions of terrestrial ecosystems at the regional scale, at a spatial resolution of several tens of meters and independent of cloud cover and vegetation type.

INTRODUCTION

Freeze–thaw cycles play a major role in high latitude terrestrial ecosystems. Freezing and frost drought result in potential damage to living plants and have a profound effect on the natural distribution of vegetation types and on their proliferation (Burke et al., 1976). Freezing and thawing also produce large changes in heat balance between land and atmosphere during spring break-up and fall freeze-up, and dissipate more than half the annual heat balance in the Arctic (Weller and Holmgren, 1974). More importantly, annual freeze/thaw cycles determine the length of the growing season for vegetation (Larcher, 1980). Knowing the length of the growing season is important for estimating annual productivity in boreal forests and in the tundra, and for understanding biogeochemical seasonal and interannual cycles such as the exchange of atmospheric CO_2 with the northern high latitude terrestrial biosphere (Houghton, 1987; Tans et al., 1990; Sundquist, 1993).

A technique for estimating the length of the growing season is to assume that photosynthetic activity is effectively halted when air temperatures drop below $-2°C$ (Waring et al., 1994). For close canopy forests, canopy temperatures are within a few degrees of air temperature (Luvall and Holbo, 1989) and can be estimated using thermal infrared emissions gathered by NOAA's Advanced Very High Resolution Radiometer (AVHRR). Access to these data is, however, limited by cloud cover.

Here, we investigate the possibility of measuring the length of the growing season by monitoring freeze–thaw cycles using SAR data collected by the first Euro-

[*] Jet Propulsion Laboratory, California Institute of Technology, Pasadena.

Address correspondence to Eric Rignot, Jet Propulsion Laboratory, California Institute of Technology, Mail Stop 300-243, Pasadena, CA 91109.
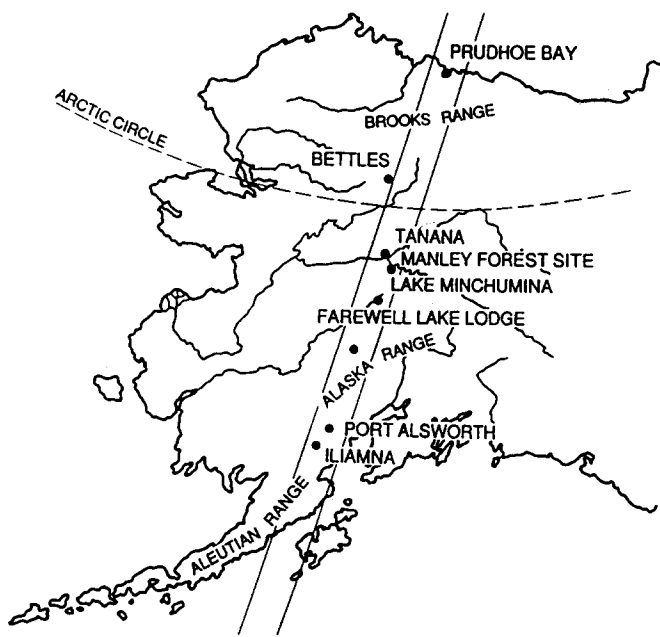
Figure 1. ERS-1 north–south Alaskan transect that intercepts with the city of Manley Hot Springs, Alaska, during the 1991 Commissioning Phase. ERS-1 is flying from top to bottom (descending pass), looking to its right, at about 1:00 p.m. Alaska daylight time. The swath width is 100 km.

pean Earth Remote Sensing satellite, ERS-1. At microwave frequencies, freezing results in a large decrease of the dielectric constant of soil and vegetation because it essentially stops the rotation of the polar water molecules contained within the soil and vegetation. Active microwave signals are directly sensitive to changes in the dielectric properties of natural surfaces. Past studies have shown the radar backscatter of frozen ground and frozen vegetation is much lower than the radar backscatter of thawed ground and vegetation (Ulaby et al., 1982; Way et al., 1990). Wegmüller (1990) measured a 3–4 dB drop in radar backscatter from bare soils during day–night freeze–thaw cycles at C-band frequency, vertical receive and transmit polarization (abrev. VV-), 23° incidence angle, that is, similar to ERS-1 radar mode. For forested areas, Rignot et al. (1994) measured a 3 dB drop in radar backscatter with freezing at a forest site in interior Alaska using ERS-1 SAR data. In this article, we present an extension of that study to the regional scale, over a broader range of terrain cover categories and climatic conditions, using SAR data from the ERS-1 SAR satellite.

METHODS

ERS-1 SAR Data

ERS-1 operates an active microwave instrument at C-band VV-polarization, 23° look angle, 100 km swath width, and 30 m resolution on the ground (Attema, 1991). The

data addressed in this article were received, processed, and calibrated by NASA's Alaska SAR Facility (ASF) at the University of Alaska's Geophysical Institute in Fairbanks, Alaska (Carsey and Weeks, 1987). The data are calibrated with an accuracy better than 1 dB (Fatland and Freeman, 1992), with a stability in calibration better than 0.33 dB (Lovet, 1993). During the Commissioning Phase of 1991, between 3 August and 15 December 1991, ERS-1 followed a sun-synchronous polar orbit at a mean altitude of 785 km with a 3-day exact repeat cycle, which provided for certain parts of the world, including Alaska, exact repeat coverage of the same areas every 3 days. In the center of Alaska, the 3-day repeat track of ERS-1 intercepted with the city of Manley Hot Springs (64°52'N, 151°20'W), Alaska (Fig. 1).

Because of the exact repeat-pass geometry, slant-range ERS-1 SAR data from the Commissioning Phase can be registered on a pixel per pixel basis using a single tie-point. Changes in radar backscatter can be measured accurately, independent of topographic variations, by computing the ratio of the radar backscatter intensities between two dates (Rignot and van Zyl, 1993). An example is shown in Fig. 2.

Environmental Parameters

Air and soil temperatures were monitored continuously in three forest stands near the city of Manley Hot Springs between August and December 1991 (Fig. 3), along with soil and vegetation moisture conditions (Rignot et al., 1994). In addition, seven National Weather Service airport weather stations located within the ERS-1 SAR transect mask provided air temperatures, daily precipitation rates, and snow depths for the entire period of observation and across the entire transect (Fig. 4). These *in situ* measurements are proxy indicators of the environmental state of the landscape, the date of onset of freezing, and the date of appearance of a permanent snow cover on the ground.

The vegetation landscape varies significantly in type, structure, and hydrologic properties across Alaska. The Arctic coastal plains north of the Brooks Range are flat areas of low elevation covered with wet tundra and marsh; the Arctic foothills south of the coastal areas are highlands of rolling topography covered with moist tundra interspersed with shrub thicklets in the river basins; barren alpine tundra dominates within the high rugged mountains of the Brooks Range; and the interior of Alaska is a mixture of plains and lowlands, covered with open, low-growing spruce forests, or closed spruce–hardwood forests, or treeless bogs.

RESULTS

ERS-1 C-band radar backscatter, σ°, from a black spruce (*Picea mariana*) stand in a forest site located near the
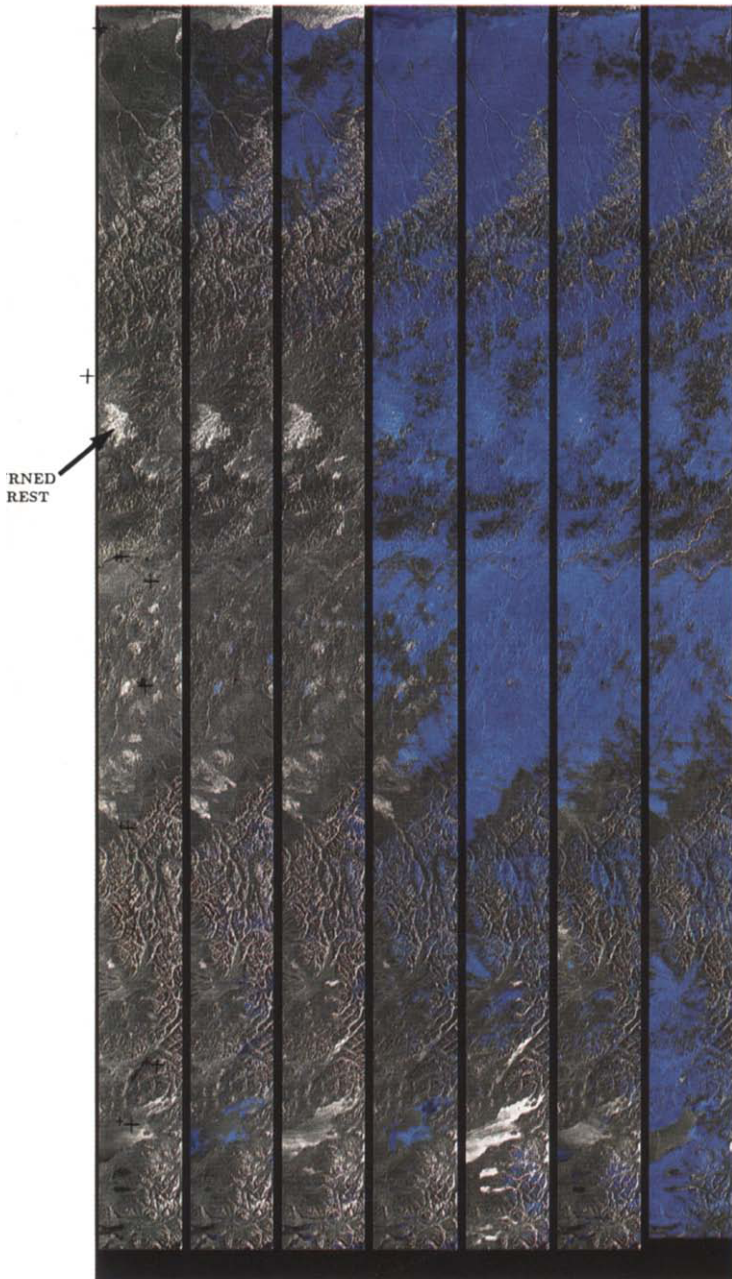
Figure 2. North–south Alaskan transects acquired by ERS-1 SAR during the 1991 Commissioning Phase. North is on top: ERS-1 is flying from top to bottom, looking to its right. Each transect is 100 km × 1400 km in size, 200-m resolution on the ground. The radar backscatter amplitude of the signal is represented in grey tone in A)–G). Areas of pronounced textural variations correspond to mountainous regions such as the Brooks Range to the North and the Alaska Range to the South. + symbols locate seven airport weather stations along the transect and the forest site near Manley Hot Springs. Also see Fig. 1. Rev #384, DOY 224 (A) is the reference transect used to compute changes in radar backscatter $\sigma°$ relative to a thawed, wet state of the landscape. In the other transects (B–G) [Rev #814 (DOY 254), 1072 (DOY 272), 1201 (DOY 281), 1330 (DOY 290), 1502 (DOY 302), and 1760 (DOY 320)] areas of decreases in $\sigma°$ larger than 3 dB are colored blue with an intensity modulation determined by the amplitude of the signal. ©ESA 1991.
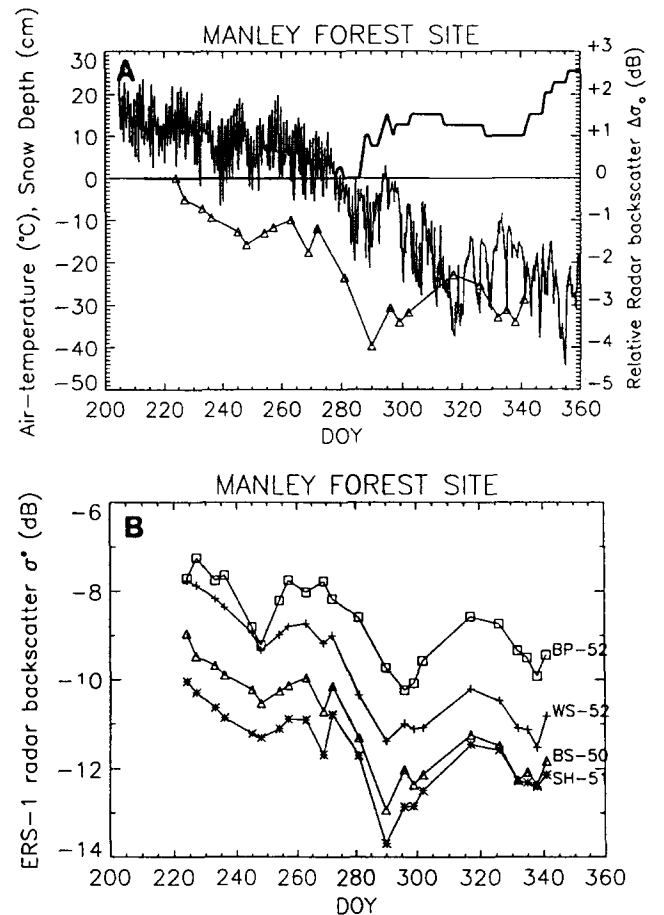

Figure 3. Air temperatures recorded in a forest site near Manley Hot Springs (64°52′N, 151°20′W), Alaska, along with ERS-1 radar backscatter measurements in A) black spruce (BS) and B) balsam poplar (BP), white spruce (WS), and treeless / bog (SH) stands. Triangles mark the dates of availability of ERS-1 SAR data.

city of Manley Hot Springs, Alaska, decreased by more than 3 dB between DOY 270, when air temperatures were warm and above zero, and DOY 290, when air temperatures fell several degrees below zero during the day and soil temperatures were below zero at 10 cm depth (Fig. 3A). A similar decrease in $\sigma°$ was observed in balsam poplar (*Populus balsamifera*) stands, white spruce (*Picea glauca*) stands, and treeless / bog stands at the same forest site (Fig. 3B). This decrease in radar backscatter has been explained by radar backscatter models and *in situ* observations of the environmental state of the trees as induced by a large decrease in the dielectric constant of soil and vegetation with freezing (Rignot et al., 1994). Between DOY 270 and 290, daily precipitation rates averaged 3 mm / day so that the drop in radar backscatter cannot be attributed to drying of the soil and vegetation. Snow appeared on DOY 280. Radar backscatter models, however, predict that fresh, dry snow is nearly transparent to ERS-1 radar signals
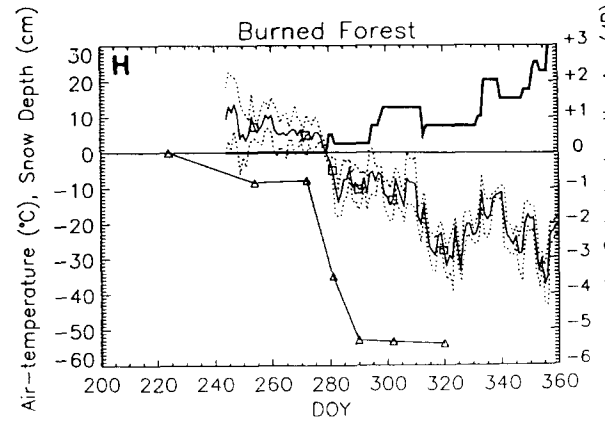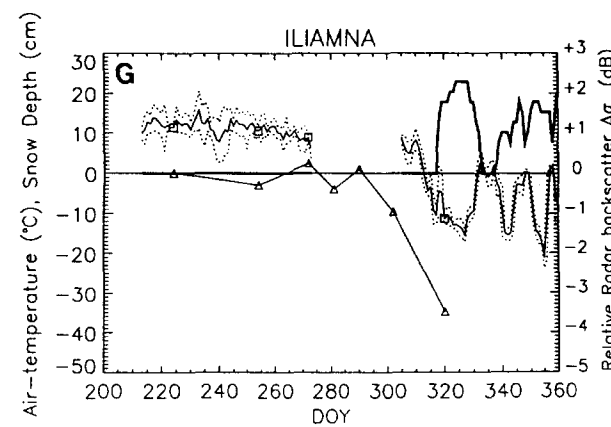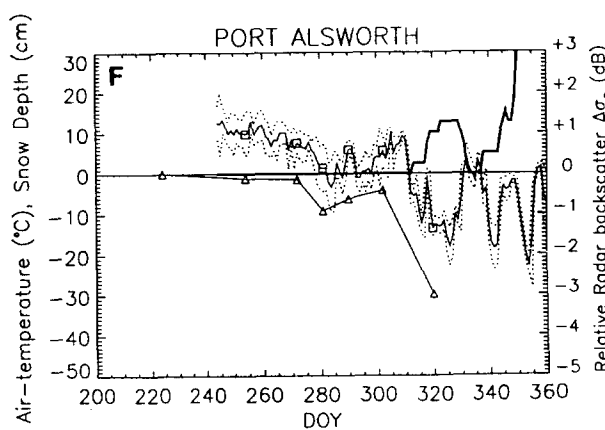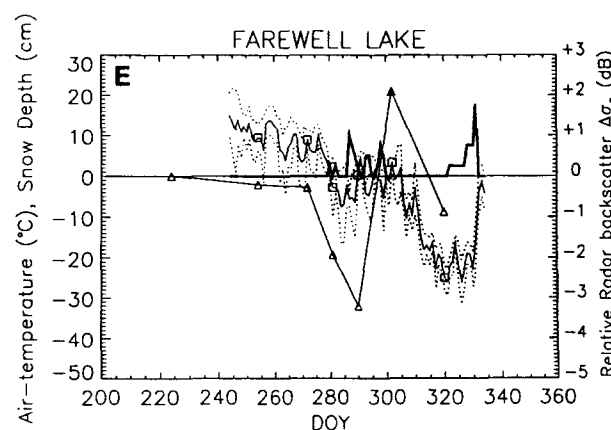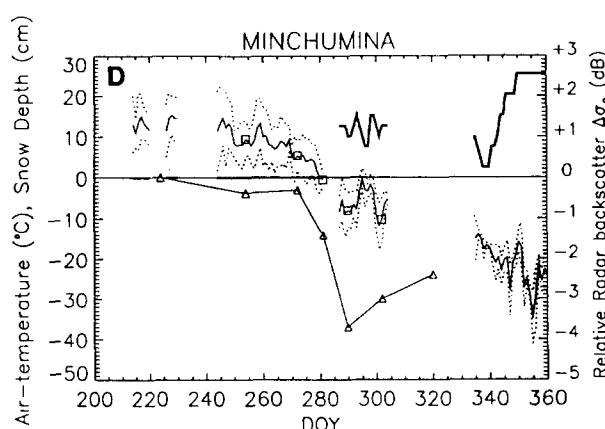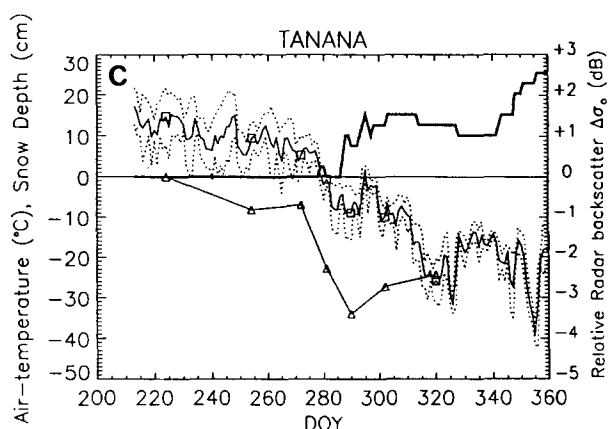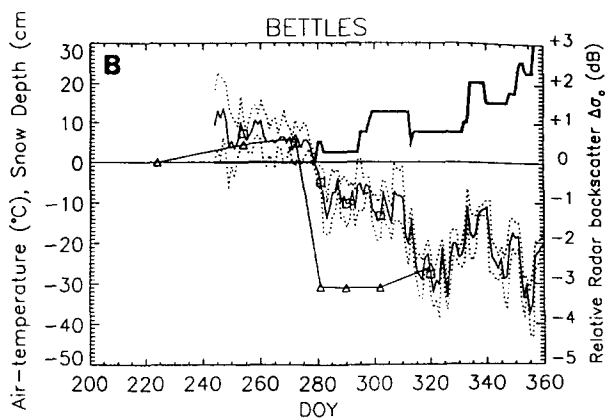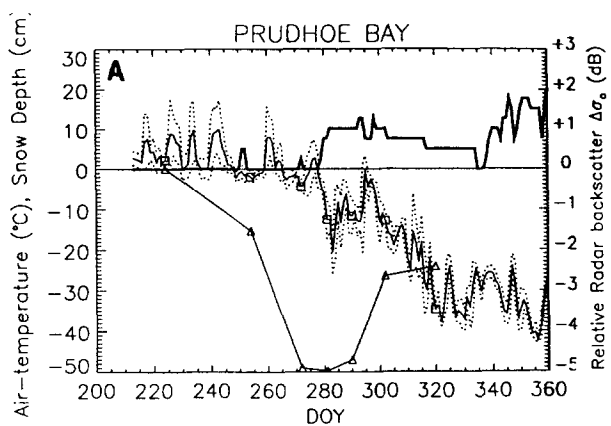
(Rignot et al., 1994). The 3 dB drop in radar backscatter therefore cannot be due to snow either. Similarly, leaves were already off deciduous trees on DOY 270 so the decrease in radar backscatter observed on DOY 280 cannot be attributed to a loss in leaf biomass.

After freezing, ERS-1 radar backscatter became positively correlated with snow depth (Fig. 3A). This increase in radar backscatter probably is due to volume scattering from large, skeletal, depth-hoar ice crystals that form at the base of the snow pack once a steady regime of cold air temperatures is established over the thin snow cover. Additional details on this theoretical interpretation are given elsewhere (Rignot et al., 1994). The radar backscatter increase is not due to thawing of the landscape.

To examine whether ERS-1 SAR could monitor changes in radar backscatter associated with freezing over larger areas, we computed the ratio of the radar backscatter intensities recorded on different dates along the north–south Alaskan transect shown in Figure 1. The results are shown in Figures 2B–G. In all the transects, the reference date is DOY 224, in the midst of the rainy season in Alaska. Daily precipitation rates recorded at airport weather stations suggest the landscape was in thawed and wet conditions at low elevations at that time. A large drop in σ° was first detected on DOY 254 north of the Brooks Range, slowly propagating through the southern latitudes thereafter, until it affected the entire transect on DOY 320.

Radar backscatter values from homogeneous areas (20 × 20 pixel square window, 2 km × 2 km in size) surrounding the seven airport weather stations were extracted for comparison with air-temperature recordings. Freezing air temperatures were recorded at Prudhoe Bay (70.15°N, − 148.20°W, 24 m elev.) at night on DOY 230 and during the day starting DOY 250 (Fig. 4A). On DOY 272, the landscape was frozen (air temperature below − 2°C) and ERS-1 radar backscatter dropped by about 5 dB relative to DOY 224. Freezing in the tundra therefore yields a more pronounced decrease in σ° than freezing in forested areas of interior Alaska. After DOY 290, snow covered the ground and σ° became positively correlated with snow depth, consistent with the observations at the Manley forest site and probably also due to volume scattering from large, skeletal depth hoar crystals. Near Bettles (66.55°N, 151.31°W, 198 m elev.), freezing occurred on DOY 278 and σ° decreased by

more than 3 dB on DOY 280 relative to DOY 224. Snow also appeared on DOY 280 but only affected ERS-1 radar backscatter values several days after, once air temperatures were well established below zero (Fig. 4B). Radar backscatter values and air temperatures recorded at Tanana (65.10°N, 152.06°W, 70 m elev.) (Fig. 4C) are consistent with those shown in Figure 3A. Freezing air temperatures were also recorded on DOY 280 at Lake Minchumina (63.54°N, 152.16°W, 213 m elev.), yielding a decrease in σ° of about 4 dB on DOY 290 relative to DOY 224 (Fig. 4D).

At Farewell Lake (62.32°N, 153.37°W, 457 m elev.), σ° decreased by more than 3 dB on DOY 290 compared to DOY 224 with freezing. A return of warm air temperatures subsequently increased σ° by 5 dB on DOY 302 compared to DOY 290, followed by a decrease of about 3 dB on DOY 320 compared to DOY 302 with the return of cold weather conditions (Fig. 4E). As σ° did not return to its DOY 224 level on DOY 302 with the return of thawed conditions, most likely because snow melt increased the amount of water in the ground layers, the decrease in radar backscatter between DOY 224 and DOY 320 was only of 1 dB, that is, not sufficient to detect freezing based on a single reference date. The two freeze / thaw transitions, however, appear clearly in the time series of radar backscatter measurements. At Port Alsworth (60.12°N, 154.18°W, 79 m), freezing air temperatures occurred on DOY 315, resulting in a 3 dB decrease in σ° on DOY 320 (Fig. 4F). The cold air temperatures recorded on DOY 280 at night only yielded a 1 dB decrease in radar backscatter, suggesting that they were not cold enough to reduce significantly the dielectric properties of the soil and vegetation. The results observed at Iliamna (59.45°N, 154.55°W, 58 m) are similar, with a decrease in σ° greater than 3 dB with freezing (Fig. 4G).

In summary, areas where σ° decreased by more than 3 dB compared to its DOY 224 level (colored blue in Fig. 2) correspond very well with areas where the vegetation and ground layers froze. The magnitude of the decrease in σ° with freezing is actually greater in the tundra than in the forest, but areas of freeze are still detected successfully independent of the type of vegetation cover when considering the minimum change, that is, a 3 dB drop in radar backscatter. In areas of successive freeze / thaw events, where the water status of the soil and vegetation changes significantly in be-

Figure 4. Air temperatures (minimum and maximum are dotted lines; average of the two is a continuous line) and snow depth (thick continuous line) recorded at seven airport weather stations between DOY 214 and 360 along with the radar backscatter values measured by ERS-1 SAR in homogeneous areas surrounding the weather stations. The dates of availability of ERS-1 data are shown as squares on the average air-temperature curves and as triangles on the radar backscatter curves. A) Prudhoe bay; B) Bettles; C) Tanana; D) Minchumina; E) Farewell Lake; F) Port Alsworth; G) Iliamna. Blanks indicate missing data. H) Burned forest with snow depth and air temperature recorded at Bettles, Alaska. The location of the burned forest stand is given in Figure 2A.

tween two cycles, for instance, because of snow melt, time series of radar backscatter measurements are required to detect successive freezing events since changes detected based on a single reference date may be limited to the detection of the first freezing event.

Several features of interest appear in Figure 2. The radar backscatter from river channels in the Arctic Plains (top) and in interior Alaska (center) increases with freezing. This effect can be interpreted as resulting from the formation of a rough, jagged ice–water interface with freezing, which increases the refraction of the radar signals at the air–ice interface, thereby steepening the incidence angle and increasing radar backscatter from the surface, combined with a shortening of the radar wavelength in the water–ice medium which increases the roughness of the ice–water interface at the wavelength scale and thereby enhances radar backscatter from the interface. For lakes, on the contrary, $\sigma°$ may first decrease because scattering off a rough, wind-exposed air–water interface is replaced by scattering off a smooth, ice–water interface. Later on, $\sigma°$ increases due to additional forward scattering off air-bubble inclusions slowly forming within the lake ice (Jeffries et al., 1992). Clearly, the simple change detection technique described in this article does not apply to open water areas.

No changes in $\sigma°$ are detected at high elevation in the Brooks Range (Fig. 2). With air temperatures of about 2°C in Prudhoe Bay (24 m elev.) on DOY 224 and a dry adiabatic lapse rate of 1°C / 100 m, subzero air temperatures probably already reigned above 224 m elevation on DOY 224, where most of the Brooks Range lay, which explains why $\sigma°$ remained fairly constant. Similarly, the highest mountains of the Alaska Range, south of Farewell Lake, do not show any decrease in radar backscatter from DOY 224 to DOY 320, probably for the same reason.

Recently burned forests appear very bright to ERS-1 SAR. This effect probably is due to enhanced forward scattering of radar signals through double bounce interactions between the tree trunks deprived of branches and the ground floor (Kasischke et al., 1992), possibly combined with the fact that the ground moisture increases significantly after burning (Kasischke, private communication). An example location is shown on Figure 2A, with corresponding radar backscatter values shown in Figure 4H. The rate of decrease of $\sigma°$ in this area is lower than in the surrounding areas (Fig. 4B), suggesting that recently burned areas take longer to freeze. Interestingly, when a fire burns in a northern black spruce forest underlain by permafrost, the thickness of the active layer (i.e, portion of the ground above the permafrost that thaws annually) increases, not because of the heat of the fire, but because of the removal of the insulating organic material, which lowers the surface albedo and decreases shading effects of

the tree canopy (Viereck and Elbert, 1972). As the underlying permafrost partially thaws, the ground layers become wetter. Hence, freeze-up of ground layers is expected to take longer in burned forests, thereby explaining why the rate of decrease of $\sigma°$ is lower there compared to surrounding areas. This example illustrates the dependence of freezing rates on the amount of soil moisture in the soil profile as discussed in Drew et al. (1958) and Luthin and Guymon (1974), and suggests repeat-pass SAR imagery could also detect differences in freezing rates of the landscape associated with differences in the amount of liquid water available at the surface.

CONCLUSIONS

This article presents a simple change detection technique for monitoring freeze–thaw cycles in northern high latitude terrestrial ecosystems using repeat-pass ERS-1 SAR data. The results indicate ERS-1 SAR could monitor freeze-up of the landscape independent of the type of surface cover over very large areas. The SAR results are in good agreement with subzero air temperatures collected at a forest site in interior Alaska and at airport weather stations across the entire state. Monitoring freeze–thaw at those latitudes could help determine the length of the growing season within a few days at the regional / continental scale, which would be very useful for estimating annual productivity in boreal forests and in the tundra and for improving our understanding and modeling of land–atmosphere interactions and biogeochemical cycling.

With the single-polarization, single-frequency SAR data provided by ERS-1, soil and vegetation are considered here as a single medium which undergoes large freeze–thaw cycles. Further studies are required to determine whether by adding SAR data acquired at another frequency, for example, L-band frequency (λ = 24 cm) from the Japanese J-ERS-1 satellite launched in 1992, we could also determine which constituents of the soil and vegetation layers freeze or thaw first. Such information could improve the determination of potential frost damage to the vegetation (dependent on canopy thaw with soil remaining frozen) as well as the start of the growing season (dependent on soil thaw).

In spring, ERS-1 radar backscatter is expected to increase when the soil and vegetation thaw, but the electromagnetic response of the surface could be complicated by the presence of melting snow in various spatial patterns and by the rapidly changing and growing vegetation. Also, in its current phase of observation, ERS-1 only provides exact repeat coverage every 35 days and approximate repeat coverage every 7–14 days, depending on latitude, thereby limiting the determination of the start of the growing season to 1–2 weeks.

REFERENCES

Attema, E. (1991), The active microwave instrument on-board the ERS-1 satellite, *Proc. IEEE* 79:791–799.

Burke, M. J., Gusta, L. V., Quamme, H. A., Weiser, C. J., and P. H. Li (1976), Freezing and injury in plants, *Ann. Rev. Plant. Physiol.* 27:507–28.

Carsey, F., and Weeks, W. (1987), The planned Alaska SAR Facility: an overview, in *Proc. of the 1987 Int. Geosci. and Remote Sens. Symp.*, IEEE Cat. 87CH2434-9, Ann Arbor, MI, 18–21 May, IEEE, New York, pp. 1059–1062.

Drew, J. V., Tedro, J. C. F., Shanks, R. E., and Korando, J. J. (1958), Rate and depth of thaw in arctic soils, *Trans. Am. Geophys. Union* 39:697–701.

Fatland, D. R., and Freeman, A. (1992), Calibration and change detection using Alaska SAR Facility ERS-1 SAR data, in *Proc. of the 1992 IEEE Int. Geosci. and Remote Sens. Symp.*, Houston, TX, 26–29 May, IEEE, New York, pp. 1164–1166.

Houghton, R. A. (1987), Biotic changes consistent with the increased seasonal amplitude of atmospheric CO_2 concentrations, *J. Geophys. Res.* 92:4223–4230.

Jeffries, M. O., Wakabayashi, H., and Weeks, W. F. (1992), C-band SAR backscatter from ice on shallow tundra lakes: observations and modeling, in *Proc. First ERS-1 Symposium*, ESA SP-359, European Space Agency, Paris, p. 91.

Kasischke, E. S., Bourgeau-Chavez, L. L., French, N. H., Harrell, P., and Christensen, N. L. (1992), Initial observations on the use of SAR imagery to monitor wildfires in Boreal forests, *Int. J. Remote Sens.* 13:3495–3502.

Larcher, W. (1980), *Physiological Plant Ecology*, Springer-Verlag, New York, p. 116.

Lovet, J. (1993), ERS-1: 18 months in orbit, in *Proc. Third Spaceborne Imaging Radar Symposium*, JPL 93-16, Jet Propulsion Laboratory, Pasadena, CA, p. 9.

Luthin, J. N., and Guymon, G. L. (1974), Soil moisture–vegetation–temperature relationships in central Alaska, *J. Hydrol.* 23:233–246.

Luvall, J. C., and Holbo, H. R. (1989), Measurements of short-term thermal responses of coniferous forest canopies using thermal scanner data, *Remote Sens. Environ.* 27:1–10.

Rignot, E., and van Zyl, J. J. (1993), Change detection techniques for ERS-1 SAR, *IEEE Trans. Geosci. Remote Sens.* 31:896–906.

Rignot, E., Way, J. B., McDonald, K., et al. (1994), Monitoring of environmental conditions in taiga forests using ERS-1 SAR, *Remote Sens. Environ.*, 49:155–164.

Sundquist, E. T. (1993), The global carbon dioxide budget, *Science* 259:934–941.

Tans, P. P., Fung, I. Y., and Takahashi, T. (1990), Observational constraints on the global atmospheric CO_2 budget, *Science* 247:1431–1438.

Ulaby, F. T., Moore, R. K., and Fung, A. K. (1981, 1982, 1986), *Microwave Remote Sensing*, Artech House, Dedham, MA, Vol. 1 (1981), Vol. 2 (1982), Vol. 3 (1986).

Viereck, L. A., and Elbert, L. L. (1972), *Alaska Trees and Shrubs*, Agriculture Handbook No. 410, Forest Service, U.S. Dept. of Agriculture, Washington, D.C.

Waring, R. H., Runyon, J., Goward, S. N., McCreight, R., Yoder, B., and Rayan, M. G. (1994), Developing remote sensing techniques to estimate photosynthesis and annual forest growth across a steep climatic gradient in western Oregon, USA, *Studia Forestalia Suecica*, forthcoming.

Way, J. B., Paris, J., Kasischke, E., et al. (1990), The effect of changing environmental conditions on microwave signatures of forest ecosystems: preliminary results of the March 1988 Alaskan aircraft SAR experiment, *Int. J. Remote Sens.* 11:1119–1144.

Weller, G., and Holmgren, B. (1974), The microclimates of the arctic tundra, *J. Appl. Meteorol.* 13:854–862.

Wegmüller, U. (1900), The effect of freezing and thawing on the microwave signatures of bare soil, *Remote Sens. Environ.*, 33:123–135.